Indian Journal of Science and Technology, *DOI: 10.17485/ijst/2016/v9i1/75243 2015*

ISSN (Print) : 0974-6846
ISSN (Online) : 0974-5645

CAD for Lung Nodule Detection in Chest Radiography using Complex Wavelet Transform and Shearlet Transform Features

M. Mercy Theresa[1*] and V. Subbiah Bharathi[2]

[1]Faculty of Electronics and Communication Engineering, Sathyabama University, Chennai – 600119, Tamil Nadu, India; mercyjesudossa@gmail.com
[2]S. R. M. University, Chennai – 603203, Tamil Nadu, India; yughasurya@yahoo.co.in

Abstract

Background and Objectives: The main objective of this paper is to extract the lung nodules in Chest Radiography (CR) for identifying and locating the presence of small lesion or nodules. **Methods and Statistical Analysis:** Four stages of works are carried out such as: 1). Image Registration using geometrical transformation method, 2). Lung Segmentation using thresholding method, 3). Feature Extraction using Complex Wavelet Transformation method and Shearlet transformation method and finally 4). Image Classification using Random Forest method and classify the images are normal or abnormal. To confirm the abnormality of the segmented output the results are compared with the labeled ground truth images given by medical experts. Findings:The entire proposed approach is implemented in MATLAB software and the performance is verified by comparing the results obtained from CWT results with the ST results. The proposed experiment is carried out on JSRT dataset and obtained the accuracy 96% which is better than the existing approach's obtained accuracy is 95.4%. Conclusion and Improvements: The proposed approach in this paper is better than the existing approaches for lung nodule detection and identification through segmentation in chest radiography. In future work the performance of the proposed work is evaluated by comparing the obtained results with the other existing transformation methods.

Keywords: Chest Radiography, Complex Wavelet Transformation, Lung Nodule Detection, Shearlet Transformation, CAD

1. Introduction

The Chest Radiography (CXR) imaging technique is used for diagnosing various abnormalities in the chest region. The diagnosis of the CXR depends on the segmentation of different anatomical structures such as bones, ribs, clavicles, heart and lungs. Eventhough Computed Tomography (CT) is superior to CXR in diagnosing abnormality in the chest, CXR is cost effective. Hence it is important to evaluate the performance of the algorithm, that extract the abnormality features correctly for the CXR based imaging. Usually the different region of chest consists of five different types of densities such as air, fat, soft tissue, bone and metal. The variation in the intensities of the CXR shows the presence of this different intensities[1]. In this Paper, we aim at segmenting and finding the abnormality in the lung region. The normal lung appears black since it is filled with air. Abnormality in the lung region can be easily identified by the presence of white or gray intensity. Automatic detection of Lung Nodule (LN) in chest radiography is the important task because the presence of lung nodule may be the symptom of cancer or Tuberculosis. One third of the population of the world is exposed to various lung abnormalities in each year. Various innovative hardware and software methodologies are proposed for LN detection[2]. Computer Aided Diagnosis (CAD) for analyzing lung nodule helps the radiologist to identify the disease

**Author for correspondence*

earlier than conventional diagnosis techniques. A number of techniques have been available for segmenting the lung from CXR to diagnose lung cancer[3]. We are using thresholding techniques for segmenting lung region and global thresholding for segmenting lung nodules which give good results. Lung nodule segmentation is a critical task if nodule size is very small. In this paper, we use the multiresolution method for feature extraction which gives better feature set for classification when compared to feature set extracted using the spatial domain Method[4].

Some of the other companies developed similar machines and software was developed for diagnoses the LN , but the sensitivity is not perfect[5]. Figure 1 depicts the chest radiographs of subject with LN. It has been proved using a positive culture test. A subtle abnormality in the upper left lung near the mediastinum is depicted in the left image, whereas the abnormalities in the hilar region are depicted in the middle image. The right image only shows obvious patchy abnormalities indicative of LN[6].

Chest radiography is mostly used for testing LN based normality or abnormality. WHO (World Health Organization) has found more difficulties in the 1960s regarding LN patients in the initial stage. Then they used X-Ray in cheap and easy way for finding the digital chest radiography. After WHO, digital chest radiography is used in large potential manner for LN diagnosis. Testing X-ray by experts is not feasible all the time afforded. LN suspects after screening the symptoms in chest radiography. MC (Montgomery County chest X-ray set) is used as training data sets for testing the LN by using segmentation algorithms[7]. If pulmonary LN increases, then it increases the HIV (Human Immunodeficiency Virus) infection rate[8]. In most of the diagnostic conditions, appropriate images are used for segmenting and extracting the lung boundaries. Various types of analysis were used using various measurements like volume, shape and size. These measurements can provide a decision about series diseases such as emphysema[9], cardiomegaly, pneumothorax or pneumoconiosis. Some authors developed CAD systems for identifying the lung diseases more accurately using lung boundary segmentation[10]. But in this paper, we proposed automatic lung segmentation and diagnosing method for chest radiography[11].

It is essential for the health society to take immediate, accurate decisions and automatically by a computer aided design. This problem is tackled in this paper by providing a sequence of image processing steps as a challenge to provide a better solution to the medical industry[12]. Figure 1 shows the overall functionalities carried out in the proposed approach. The main contribution of the proposed approach in this paper is:

- Image Registration
- Image Preprocessing
- Lung Segmentation using the Iterative Threshold method
- Feature extraction using CWT method
- Feature extraction using Shearlet method
- Comparing features with the features of the ground truth images.
- Performance evaluation by comparing the results obtained from CWT and Shearlet.

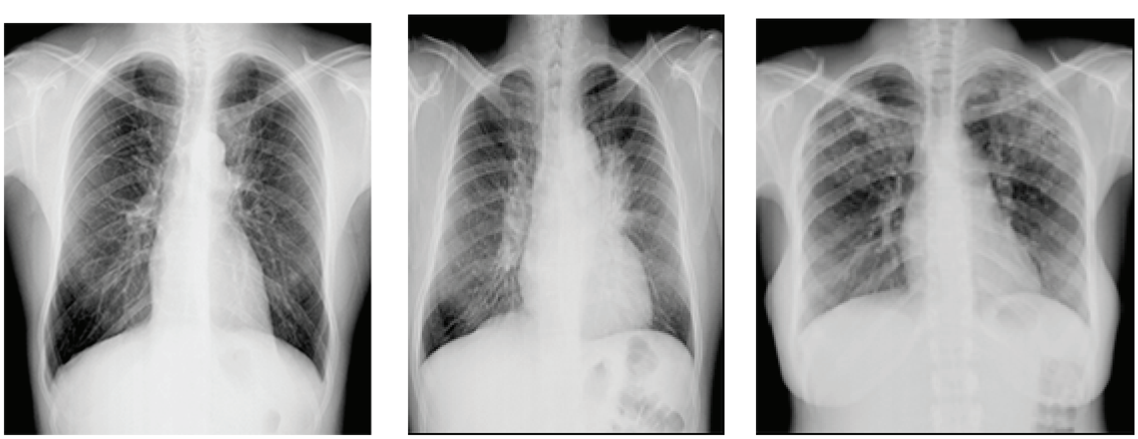

Figure 1. Chest radiography.

2. Image Registration

Image registration[13] is necessary to correct the geometrical transformations for the input images by adjusting the alignment. It is also arranging the object physically in the space. Medical images (3D) are obtained by CT, MRI (Magnetic Resonance Imaging), SPECT (Single-Photon Emission Computed Tomography) and PET (Positron Emission Tomography) where these images are a collection of continuous two dimensional images and having high intensity. Two dimensional medical images are obtained by X-ray, taken as, a film (digital radiography) gets as a photograph or a film. In all the above imaging techniques, due to the hardware resource, position of patient the image view is rotated a while. The benefit of the registration provides an accurate diagnosis or treatment and clinically makes a meaning[14]. Registration can be obtained by two images where one is the reference image and the other image is the target image. According to one another, the images can be fused or the orientation of the image is changed.

In this paper a geometrical transformation method is applied to the image for image registration. Each view of the image is correlated to the coordinate systems which defines a plane for the view. In geometrical transformation, the points in the reference image are mapped with the points on the input image and the points on the space X. The transformation T is applied in terms of reference points Y and it produces the transformed points X' as:

$$X' = T(X) \tag{1}$$

From (1), if, all the points y in Y, corresponds to x in X, then the successful image registration can provide X'. The set of all non-zero elements $T(X) - y$ is the registration error.

3. Image Preprocessing

Most of the CAD system utilizes a sequence of image processing steps (especially, preprocessing) to an input image. The key feature of the image preprocessing step is to improve image quality to obtain the segmentation results accurately. Quality of the image strongly affects the performance of the other following image processing steps in the proposed approach. In this paper, the preprocessing steps are contrast enhancement and bone suppression. Using contrast enhancement the contrast color of the X-ray image can be improved significantly where it helps to identify the tissue surface and the lung boundary more accurately. To do this, histogram analysis method is applied on the image data. Histogram equalization method increases the contrast region from the low-contrast region using the intensity values.

Another important preprocessing method specially applied on X-ray images is bone suppression. The bone suppression method eliminates the occlusion abnormalities in the lung region and improves the feature extraction quality of the CAD systems. The strong edges produce local minima and reduce the accuracy of the segmentation algorithms. In case of low resolution based input images the suppression helps to suppress the rib cage with edges of the clavicle bones. Even though, the bone suppression is a simple solution, it is more suitable for the lung segmentation and it is not suitable for other image processing steps. Bone suppression automatically removes the bone structure in the X-ray images, which helps to detect the LN accurately.

4. Lung Nodule Segmentation using Thresholding Method

An automatic lung nodule detection system is considered as an advantage for detecting the lung abnormalities at an early stage. The basic layout of the system is shown in Figure 2.

Initially the lung region is segmented and extracted from the X-Ray image by performing thresholding and a few binary reconstruction processes. Then from the extracted lung region, the nodules can be extracted by using global thresholding methods and it is used for feature extraction. The CWT and Shearlet transform methods extract the features like geometric, intensity based statistical and location based features. Finally the extracted features are classified using Random Forest classification method, to find out normal or abnormal.

Figure 3 shows an overview of segmenting lung nodule segmentation scheme. In the following sections, each stage is described in detail. Lung region segmentation is an essential preprocessing step in lung nodule detection systems. The main purpose of lung segmentation is to separate the voxels corresponding to the lung cavity in axial CT scan slices from the surrounding lung anatomy. As such, the accuracy of lung segmentation largely influences the nodule detection results. Our proposed CAD system includes a fully automated method for segmenting lung regions in CXR: global Thresholding is used to obtain the lung region and the thin structures.

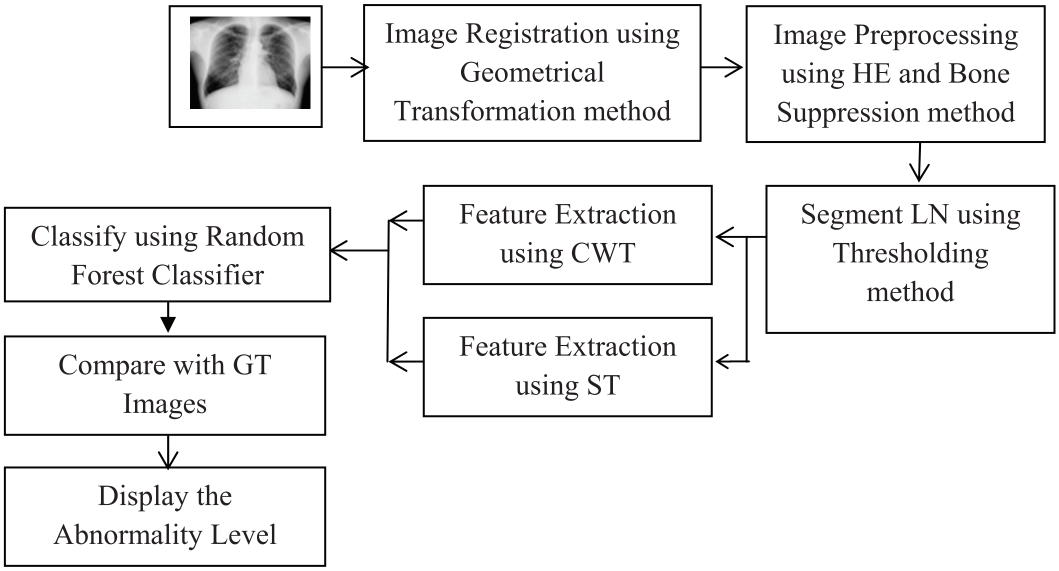

Figure 2. Proposed model.

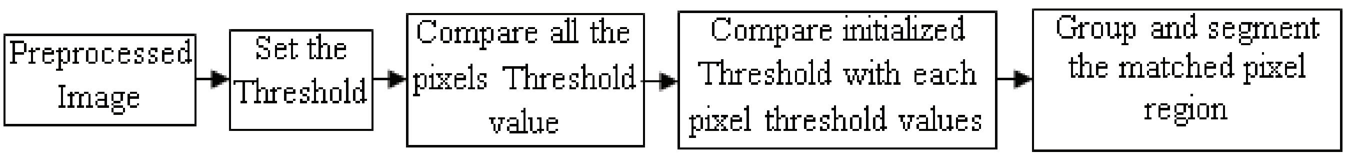

Figure 3. Thresholding based segmentation.

The X-Ray image is divided into two types as high density and low density pixels. The high density pixels mainly consist of the body neighboring around the lung cavity, whereas the low density regions consists the lung cavity. To segment and extract the lung volume it is essential to segment the low-density regions in the initial stage. First a fixed threshold value is assigned to separate the low density lung parenchyma from the overall lung anatomy. The availability of different scanning protocols makes the selection of an appropriate threshold a challenging task. The appropriate threshold is selected using global thresholding algorithm. So that, after smearing a fixed threshold T_0, subsequent process is used to improve the preliminary segmentation results.

A threshold $I(x,y)$ is defined as:

$$I(x,y) = \left\{ \begin{matrix} 1 \ if \ \ I(x,y) < T \\ 0 \ if \ \ I(x,y) \geq T \end{matrix} \right\} \quad (2)$$

The following procedure is the main approach applied for thresholding based lung nodule segmentation.

1. Initialize T_0.
2. Segment Lungs Portion using T. There are two group of pixels were categorized as Group 1 and Group 2.
3. where G1 contains the pixels threshold value < T
4. where G2 contains the pixels threshold value^3 T
5. Compute the average threshold value as m_1 and m_2 for pixels in Group1 and Group2.
6. Compute the Global Threshold value $T = \frac{1}{2}(\mu_1 + \mu_2)$
7. Repeat the above steps 2 to 4 until fetch the difference in T in successive iterations which is smaller than a predefined parameter T_0

In all kinds of segmentation based image processing, it is necessary to consider about the background image in terms of foreground objects. To separate the foreground objects a best initial threshold value is assigned for T, which is the average gray level of the image. T_0 is used to stop the algorithm after changing the value several times and obtain the appropriate lung nodule region completely. The experimental threshold value assigned to T_0 is given in Table 1. According to the threshold T_0 given in Table

1, the lung region is detected from the original X-RAY image. A binary reconstruction operation is applied after thresholding to extract the lung nodule region alone.

Table 1. T_0 value assigned for lung region extraction

Images	Threshold Value
JPCLN01.IMG	78
JPCLN03.IMG	86
JPCLN07.IMG	69

After successful segmentation, the lung nodule features are extracted using CWT and Shearlet transform method for classifying the abnormality of the lung images. The series of images tested in Table 1 is taken from JSRT (Japanese Society of Radiological Technology) image data set.

5. Finding and Detecting LN Occurrence

For successful lung nodule segmentation, a thresholding based extraction is applied. A dynamic threshold value is chosen using a trial and error method for segmenting the image. Initially a random sample value is assigned as the threshold for segmenting the Lung-Nodule. If the given threshold extract the exact Lung-Nodule then the same value is used otherwise, the threshold value is changed until it obtains the exact Lung-Nodule. This process is repeated on the chest X-ray image the lung portion is applied to detect and classify the Lung-Nodule.

6. Feature Extraction by CWT

$CWT(I) = \sum_{i=0}^{i=k} I_k \quad \forall k = 0,1,\ldots,m,$ where m is the total number of pixels in the segmented image input to CWT.

Similarly, $ST(I) = \sum_{i=0}^{i=J} I_k \quad \forall J = 0,1,\ldots,L,$ where L is the total number of pixels segmented and input to Shearlet transform method. Now, the features are extracted using CWT and Shearlet method for classification. Wavelet is a small wave having energy integrated with time. One of the transient tools for analyzing the time in terms of frequency is wavelet. The wavelet prototype function is adopted by the wavelet analysis and it is called as "Analyzing Wavelet" or "Mother Wavelet". Temporal analysis is performed using a dilated function with low frequency of the same wavelet. The mathematical formulation of the signal processing can be obtained by wallet, which provides wavelet transformation pair such as FT (Fourier Transform) and WT (Wavelet Transform).

One of the extended versions of the standard DWT (Discrete Wavelet Transform) is CWT. Since, CWT is a two-dimensional WT, it can provide sparse representation, multi resolution and beneficiary characterization of the structure of the image. CWT was introduced to overcome the limitations of the classical DWT. The high degree of the shift invariants are purveyed in terms of magnitude values. But DWT is not good in reducing the redundancy of the magnitude values. CWT uses the DWT as well as DT (Discrete Time) DWT functions. Complex wavelet transform uses analytical filter which decomposes the real-complex signals into two parts as real and imaginary portions in the transformation domain. The energy localization of the wavelet basis is described by amplitude and phase information, and is computed using real and imaginary coefficients. Complex wavelet transform provides a directional information scale of the domain exists. Morlet and Cauchy wavelets are the two main examples of CWT. A CWT $\psi(t)$ should satisfy the properties as:

$$\Psi(\omega) = \Psi^{+} + \Psi^{-}, \Psi(\omega) = \begin{Bmatrix} \Psi^{+} if \ a > 0 \\ \Psi^{-} if \ a < 0 \end{Bmatrix}$$

The Complex Morlet wavelet shown in Figure 4 is written as:

$$\psi\left(\frac{t}{a}\right) = e^{i\omega_0 t/a} e^{-t^2/2a^2}, \psi(\omega) \begin{Bmatrix} |a|\sqrt{2\pi e^{\frac{-(\omega_0 - a\omega)^2}{2}}} \quad H(\omega),\ a > 0 \\ |a|\sqrt{2\pi e^{\frac{-(\omega_0 - a\omega)^2}{2}}} \quad H(\omega),\ a < 0 \end{Bmatrix}$$

The Complex Cauchy wavelet is written as:

$$\psi\left(\frac{t}{a}\right) = \frac{\Gamma(m+1)}{2\pi}\left(1 - i\frac{t}{a}\right)^{-(m+1)},$$

$$\Psi(\omega) = \begin{Bmatrix} a^{m+1}\omega^m e^{-a\omega} H(\omega), \quad a > 0 \\ a^{m+1} - \omega^m e^{-a\omega} H(-\omega),\ a < 0 \end{Bmatrix}$$

$$\Gamma(m) = \int_0^{+\infty} t^{m-1} e^{-t} dt,\ H(\omega) = \begin{Bmatrix} 1,\ \omega > 0 \\ 0,\ \omega < 0 \end{Bmatrix}$$

CWT as shown in Figure 5 is the extension as well as an alternate complex valued extension for the standard

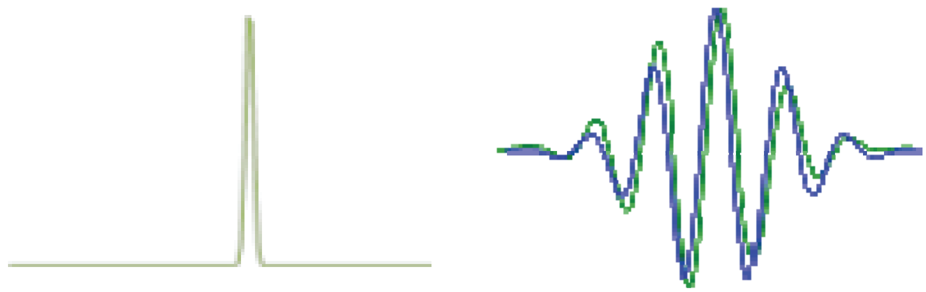

Figure 4. Morlet and normalized frequency.

DWT. The fundamental objective of the CWT is to avail explicitly both magnitude and phase information. The image is analyzed by the CWT, the phase shifts of the complex coefficients in the entire sub-band. Then the displacement vectors in each point are verified.

In this paper, it is proposed to use some of the complex symmetric daubechies wavelets which provide a natural way for calculating zero-crossings due to the hidden laplacian operator in the imaginary part of the scaling function. *Img* is the input image data, *r* is the real part and *j* is the imaginary part of *Img*. The features extracted using CWT are:

- Average
- Standard Difference
- Entropy
- Energy

In the first level down sampling, Row filter is applied and on the second level down sampling, Column Filter is applied for decomposing the image. So that, the image reconstruction will be perfect in the CWT and the result segmentation will be accurate. The main implementation transform is applied to the Mother wavelet. CWT takes all the N sample of M coefficients which are non-redundant. The CWT coefficients of the testing images in each level of decomposition are given in Table 2.

Instead of the large extraction time in terms of preceding levels as well as the larger feature vector length, for the algorithm implementation the fourth decomposition level is selected where it produces significantly smaller number of the generated coefficients than the other levels. A portion of the decomposition wavelet coefficient of the input images is shown in Table 2. Feature extraction of the segmented portion is done using the CWT for further classification and the algorithm for CWT is given in Algorithm-1:

Table 2. CWT wavelet coefficients at level l = 4

n-1	$I_0''(n-1)$	$I_1''(n-1)$	$I_2''(n-1)$	$I_3''(n-1)$
0	-0.000688	0.000856	0.0039	-0.0020
1	-0.000705	0.0018	0.0043	0.0015
2	-0.000534	0.0012	0.0029	0.00027
3	-0.000368	0.000624	-0.00067	0.0025
4	-0.000629	0.0012	0.0026	0.0024
5	-0.000711	0.0013	0.0043	-0.0028
6	-0.000544	0.000919	0.0030	-0.0019
7	-0.000338	0.000524	-0.000963	0.0080
8	-0.000619	0.0010	0.0028	0.0022
9	-0.000681	0.0012	0.0033	-0.00026
10	-0.000620	0.000951	0.0018	0.0062
11	-0.000496	0.000936	0.0036	0.0038
12	-0.000475	0.000873	0.0023	0.0065
13	-0.000617	0.0011	-0.0035	0.0057
14	-0.000228	0.000475	-0.00098	0.0039
15	-0.000620	0.0014	0.0025	-0.00029

Algorithm-1

- Select the input image
- Register the image for aligning
- Remove the noise for improving quality
- Segment the image using Threshold method
- Feature Exaction using CWT method
- Use the features for classification

7. Shearlet Based Feature Extraction

To evaluate the performance of the contour feature extraction of Lung-Nodule in this paper we utilize CWT and Shearlet transform methods. The previous section

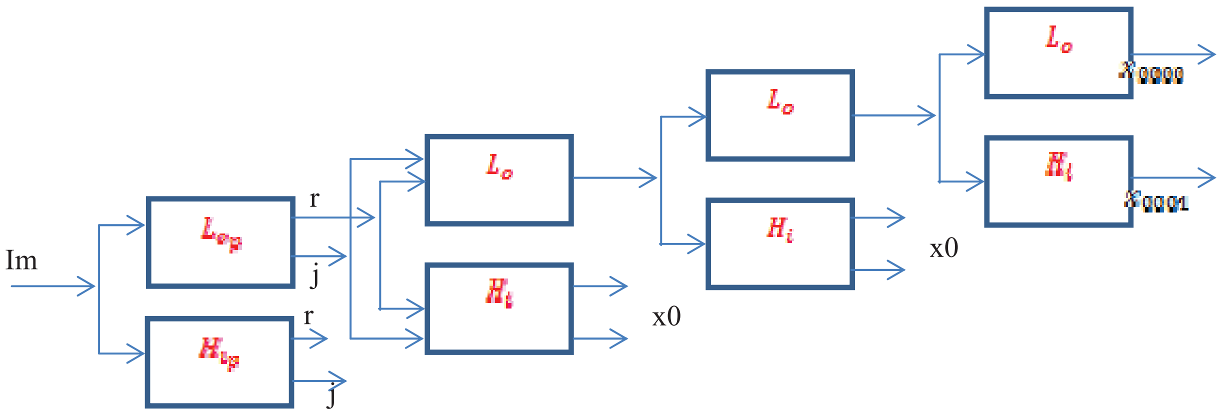

Figure 5. Complex wavelet tree.

discussed about the complex wavelet transform method. In this section we incorporate the Shearlet into a convex multi-label model. It is necessary to understand the concept of convex relaxation model in matrix-vector notation[15, 16]. The image is segmented by allocating various dissimilar labels to all the dissimilar areas of the image based on the color value or gray value of the pixels. The entire dissimilar variables are persisted in a predefined codebook. In this paper, the RGB based color values are taken for adjustment due to accurate segmentation. The image data is taken in column wise for matrix-vector notation. Accordingly, the input image $I \in \mathbb{R}^{N \times N}$ it is obtained that the vectored image $vec(I) \in \mathbb{R}^{N^2}$ where the notation I represents both the original image and reshaped image. Let $J \in \mathbb{N}$ is the number of portions in the image labeled by a list of labels in $L = \{1, 2, \ldots, J\}$.

In the given Image $\mathrm{I} \in \mathbb{R}^{\mathrm{N}^2}$ with a codebook $c = \{c_1, c_2, \ldots, c_J\}$ the labeling vector is obtained as $u^* \in \{0,1\}^{J^{N^2}}$ where it can provide a "good" segmentation of I. To make the proper interpretation it is convenient to take $u^* \in \{0,1\}^{N \times N \times J}$ as J layers of the image I in $\{0,1\}^{\mathrm{N}'\mathrm{N}}$. Generally for each pixel only the entry in one layer is 1 and the entries in the other layers are 0. At the same time, each pixel is assigned by a label according to the index of the respective layer. For the relaxation it is assumed that there should not be a restriction for non-zero entries in each layer and there should be a restriction to the sum of the overall layers for each pixel to be equal to 1. i.e., $u^* \in \{0,1\}^{J^{N^2}}$ and $u^* \sum_{k=0}^{J-1} u^*[r + kN^2] = 1 \forall 1 \le r \le N^2$. The respective label is selected according to the index of the largest entry for each pixel. The following variation approach finds u^* as the minimizer of the functional $I(u) = \langle u, s \rangle + \lambda \Psi(u)$ subject to $u \in C$ Where

$$C := \left\{ x \in [0,1]^{j^{N^2}} : \sum_{k=0}^{J-1} u^*[r + kN^2] = 1 \forall 1 \le r \le N^2 \right\}$$

The condition guarantees that the sum over all the layers of entire pixel is equal to 1. It is referred to the first terms as the data term and the second terms as regularizer and $\lambda >$ 0 as the regularization parameter. The relation between the image data I comprised in $s \in \mathbb{R}^{J^{N^2}}$ penalizes a particular distance between I and the codebook C. In all the layers I of s, we subtract the codebook value c_i from I - in formulas:

$$s[r + (k-1)N^2] = \| I(r) - c(k)_p^p \forall 1 \le r \le N^2, 1 \le k \le J.$$

Thus, for larger values of s, smaller values of the data term was attained. Due to condition $u \in C$ the trivial solution, u = 0 is excluded. The regularization term is selected to provide "smooth" layers.

In this paper, comparing with the TV-function and NL-means regularization, we used Shearlet for minimizing the functional

$$I(u) = \langle u, s \rangle + \| \wedge (I_J \otimes S \| 1 + \iota_c(u)$$

Where, I_J represents the identity matrix in $\mathbb{R}^{J \times J}$ and S is noted as the shearlet -transform applied to a vector $\mathbb{R}^{N^2}$ as depicted below

$$\left(\langle I, u_j \rangle \right)_{j=1}^{n} = UI \text{ and } I = U^T \left(\langle I, u_j \rangle \right)_{j=1}^{n}$$

In particular, we have that $S^T S = I_{N^2}$. Finally, $I_j \otimes S$ simply applies this Shearlet-transform to each layer of u separately. The indicator function l_c is defined by

$$\iota_c(u) :- \begin{Bmatrix} 0, & u \in C \\ \infty & u \notin C \end{Bmatrix}$$

Summing up, finding an appropriate labeling vector u^* for the image I is equivalent to solving the problem

$$u^* = \underset{u \in R^{J^{N^2}}}{\operatorname{argmin}} \left\{ \langle u, s \rangle + || \wedge (I_J \otimes S || 1 + \iota_c(u) \right\}$$

and it is the segmented result of I from Shearlet transform method. I consist of the set of all feature vectors. The features extracted from the Shearlet transform are:

- Mean
- Energy
- Entropy and
- STD (standard deviation) given in Table-2.

Algorithm-2:

- Select the input image
- Register the image for aligning
- Remove the noise for improving quality
- Apply Threshold method for Lung Segmentation
- Apply Shearlet Transform method for feature extraction
- Calculate the total number of black pixels in the segmented image for classification

8. Random Forest Classifier

Here, we employ a RFC (Random Forest Classifier) and it is used mostly in tracking applications, object recognition. A RFC contains numerous trees where each tree grown using some form of randomization. The leaf nodes are labeled by the posterior distribution based estimation on the image classes. Internal nodes in the tree consist a test which splits the space of the data to be classified. An input image is classified by investigating by each tree and aggregates the reaches leaf distributions. The randomness is applied at two portions during training: First by sub-sampling the training data so that each tree had been grown using a different subset and the other portion is in the selection of nodes tests.

All the trees considered in this paper are binary tree and in Top-Down structure. The way of testing each node is 1. Data independent, or 2. Using a greedy algorithm, it is tested that it best separates the given training sample image. The meaning of the best can be calculated using information gain

$$\Delta E = -\sum_i \frac{|Q_i|}{|Q|} E(Q_i)$$

caused by splitting the Q examples into two subsets as Q_i in terms of given test. Also E(q) is the entropy. This test is recursively applied to a nonterminal node in all the training samples. The recursion is stopped while it reaches a depth (which is mentioned by the user). In case, the set of all trees is T, set of classes is C and the set of all leaves is L in a given tree. While training the trees, the posterior probability ($P_{t,l}$ (Y(I) = c)) for each class c ((C at each leaf node I (L available in tree t (T. The above probabilities are calculated as per the ratio of the number of images I having c class which reaches l and to the entire images that reaches I. Y(I) is noted as the class-label c for image I.

And then test image is applied into the random-tree until it reaches the leaf-node. All posterior probabilities are then averaged and the arg – max is taken for classifying the image. For testing the images, a set of translation scales is applied. A new image W_I is classified by considering the average of the posterior probabilities ($P_{t,l}$(Y(I) = c)):

$$\hat{Y}(I) = \max_c \frac{1}{T} \sum_{t=1}^{T} (P_{t,l}(Y(I) = c))$$

where l is the leaf reached in the image I in tree t. Now it is classified that an image I as the class C_k provided by the ROI which provides the highest probability.

9. Results and Discussion

In this paper, for experimenting the proposed model there are 100 images is taken from a famous benchmark dataset and it is verified by the results obtained in step by step functionality of the proposed model. From the 100 images, 60 images are normal image and 40 images are abnormal images. Each image is taken as input image for experimenting the Algorithm-1 and Algorithm-2 which are coded in MATLAB software. The following table shows the results obtained while experimenting our proposed model. Results obtained in our proposed model are given in the Table 3. Images given in the first column show the input image used in the proposed approach, image given in the second column shows the result obtained as the result of an image enhancement process. The image given in the third column shows the detected and segmented lung image portion. The image given in the fourth column shows the Lung-Nodule analysis using threshold method. The fifth column and the six columns in the table shows the classification result obtained

Table 3. Results obtained using proposed model shown in figure 1

Input Image	Enhanced Lung Image	Detected Lung Image	Lung-Nodule	CWT Result	ST Result	GT Result
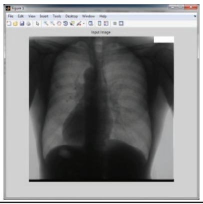	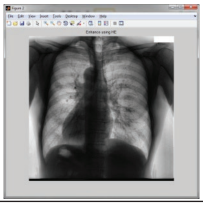	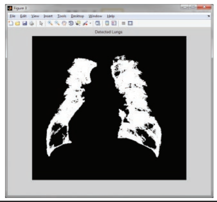	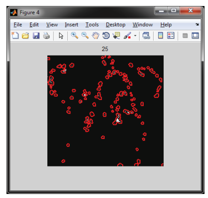	Normal	Abnormal-Benign	Benign
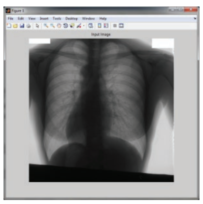	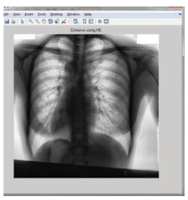	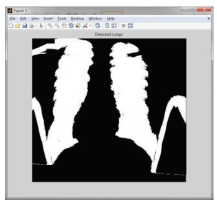	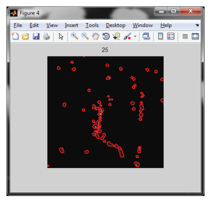	Normal	Normal	Normal
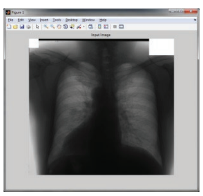	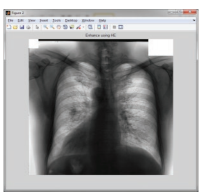	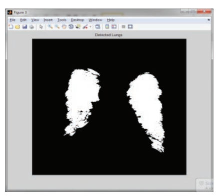	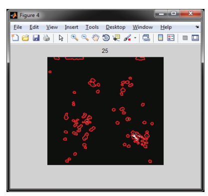	Abnormal –Benign	Abnormal-Malignant	Malignant

using complex wavelet transform and Shearlet transform respectively. The seventh column shows the real result obtained by comparing the extracted Lung-Nodule with the ground truth image based results. Then the similarity between the ground truth image and the experiment result is measured by horizontal and vertical projection profile and it can be written as:

$$sm(input_{img}, GT_{img}) = \propto \sum_{x=1}^{n} \sqrt{p1(x)p2(x)} + (1-\propto)\sum_{y=1}^{m} \sqrt{q1(y)q2(y)}$$

where p1(x) and p2(x) are the horizontal projections, q1(y) and q2(y) are the vertical projections of images $Input_{\text{img}}$ and GT_{img} respectively. x and y are the histogram bins of the projection profiles, n and m are the number of bins in the profile histogram and μ is the weight factor and it can be calculated as $\mu = n/(n+m)$ for each profile.

The feature values are extracted from the test images using CWT and Shearlet transform methods are shown in Table 5 and Table 4 respectively . Both transformation methods have an inbuilt formulation for computing and extracting the selective features from the input segmented image.

Table 4. features extracted using shearlet transform method

Images	Mean	Energy	Entropy	STD
JPCLN01.IMG	0.00519	0.0257	2.2169	0.1655
JPCLN03.IMG	0.0070	0.0248	2.3750	0.1624
JPCLN07.IMG	-0.0038	0.0083	2.3750	0.0940

10. Performance Evaluation

The segmentation performance of the system is measured with respect to the number of training images comparing with the ground truth images. In our experiment JSRT data set is used and the results are compared with the existing results. Table 6 summarizes the results obtained from the existing system as well as from our proposed system. According to the classified results obtained from

Table 5. Features extracted using complex wavelet transform method

Images	STD	Entropy	Mean	Energy
JPCLN01.IMG	0.0025	0.8112	0.00052	0.0000050
JPCLN03.IMG	0.0015	0.8113	0.00095	0.0000025
JPCLN07.IMG	0.0021	0.8113	0.00037	0.0000034

CWT, ST and GT for JSRT and Montgomery is given in Table 6.

From the Table 6, it is clear that Shearlet transform based classification in all the two datasets containing X-Ray images. Table 7 shows that the classification results obtained using complex wavelet transform in the X-Ray images. Figure 6 and Figure 7 show the result of classification of images using CWT and ST.

By comparing the results from Table 6 and Table 7, it is clear that Shearlet transform performs better than the complex wavelet transform.

Figure 8 graphically demonstrates the variation of the feature extraction time towards each of the CWT levels 1, 2, 3 and 4. As it shows, the time necessary for image feature extraction increases at each level. It is related to the required time for image energy computation by the high pass and low pass filters at each level separately. Thus, with the subsequent level the feature extraction time increases.

11. Conclusion

In this paper, complex wavelet transform based and Shearlet transform based lung boundary detection method is applied. And the obtained results are compared with the results obtained from the ground truth image. The comparison applied using similarity score computed by comparing the horizontal and vertical profile information of the images. Also the algorithms described in this paper is evaluated using two different data sets containing 100 chest radiograph images from the patients with normal as well as abnormal lung and various pulmonary diseases.

Our future work of this paper is to utilize the contour wavelet transform compared with the Curvelet transform

Table 6. Shearlet transform based classification

Dataset	Total Number of Images	Obtained Correctly	Obtained Incorrectly
JSRT	100	95	5
Montgomery.	100	96	4

Table 7. Complex wavelet transform based classification

Dataset	Total Number of Images	Obtained Correctly	Obtained Incorrectly
JSRT	100	93	7
Montgomery	100	95	5

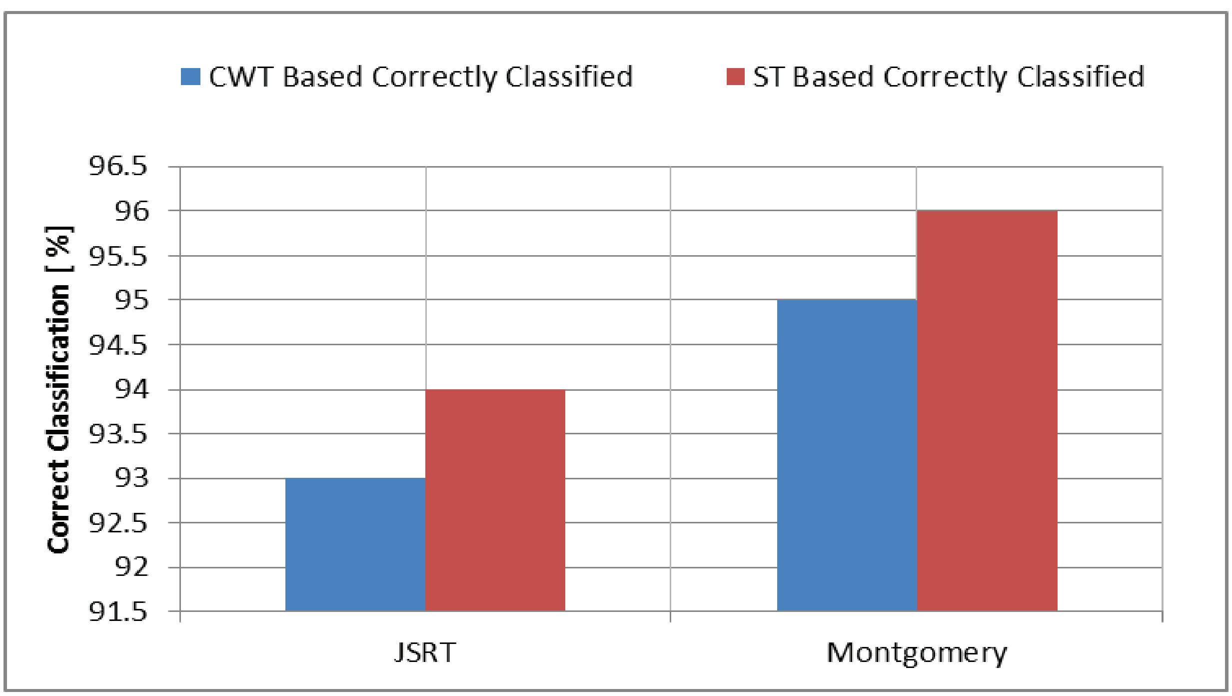

Figure 6. Number of images correctly classified by CWT and ST.

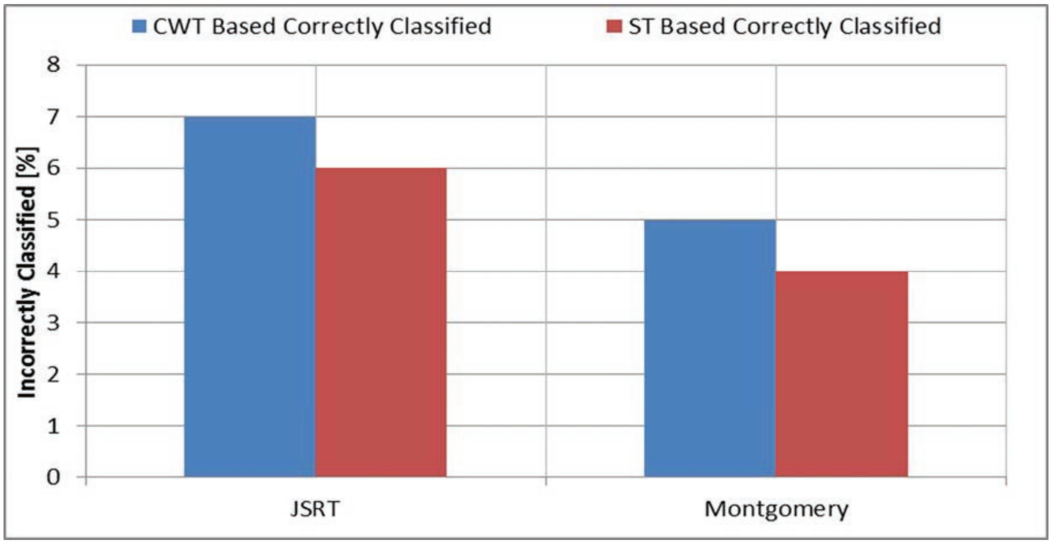

Figure 7. Number of images in-correctly classified by CWT and ST.

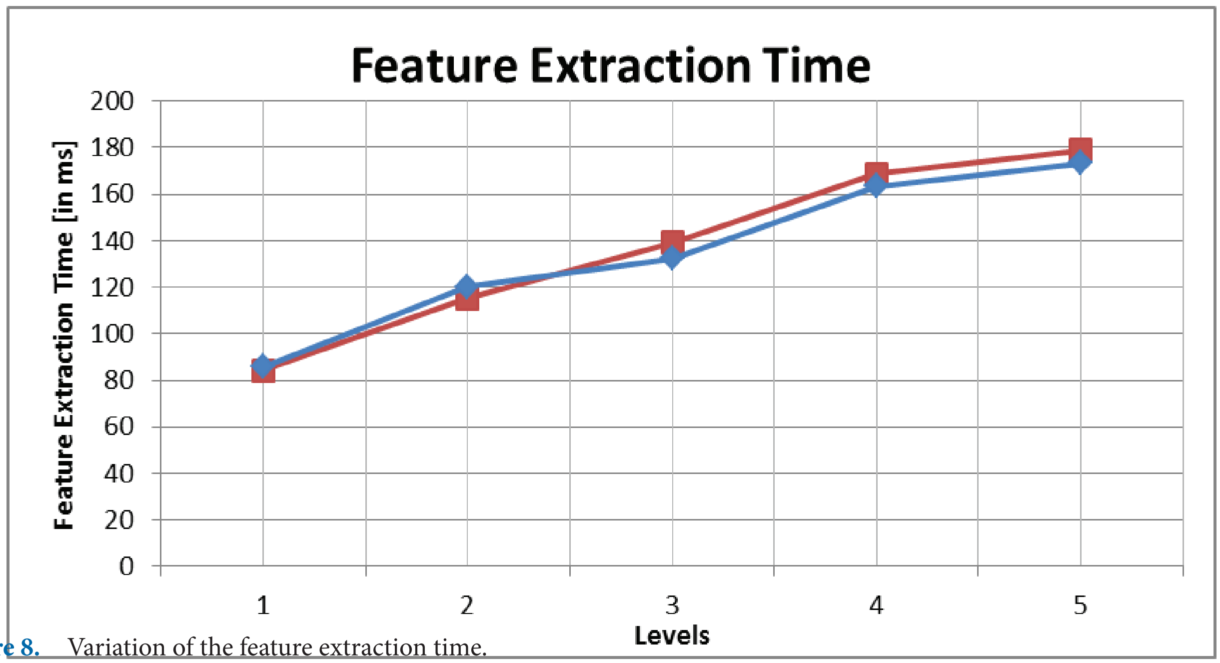

Figure 8. Variation of the feature extraction time.

based lung nodule segmentation and the effective features are compared to identify the availability of Lung-Nodule in a X-Ray chest radiogram image.

12. References

1. Hobbs DL. Chest radiography for radiologic technologists. Radiologic Technology. 2007; 78(6):491–516.
2. Carrascal FM, Carreira J, Souto M, Tahoces P, Gomez L, Vidal J. Automatic calculation of total lung capacity from automatically traced lung boundaries in postero-anterior and lateral digital chest radiographs. Medical Physics. 1998; 25(7):1118–31.
3. Dharmarajan A, Velmurugan T. Lung cancer data analysis by k-means and farthest first clustering algorithms. Indian Journal of Science and Technology. 2015 July; 8(15).

4. Lellmann J, Becker F, Schnorr C. Convex optimization for multi-class image labeling with a novel family of total variation based regularizers. IEEE International Conference on Computer Vision. 2009. p. 646–53.
5. Lellmann J, Schnorr C. Continuous multiclass labeling approaches and algorithms. SIAM Journal Imaging Science. 2010; 4(4):1049–96.
6. Miniati M, Coppini G, Monti S, Bottai M, Paterni M, Ferdeghini EM. Computer-aided recognition of emphysema on digital chestradiography. European Journal of Radiology. 2010; 80(2):169–75.
7. Taher F, Sammouda R. Lung cancer detection by using artificial neural network and fuzzy clustering methods. IEEE Conference and Exhibition (GCC). Dubai. 2011. p. 295–8.
8. Jaeger S, Karargyris A, Antani S, Toma G. Detecting Tuberculosis in radiographs using combined lung masks. International Conference on IEEE Engineering Conference on Medicine and Biology Society. California, USA. 2012. p. 4978–81.
9. Coppini G, Miniati M, Monti S, Paterni M, Favilla R, Ferdeghini EM. A computer-aided diagnosis approach for emphysema recognitionin chest radiography. Medical Engineering Physics. 2013; 35(1):63–73.
10. Jaeger S, Karargyris A, Candemir S, Sielgelman J, Folio L, Antani S, Thoma G. Automatic screening for tuberculosis in chestradiographs: A survey. Quantitative Imaging in Medicine Surery. 2013; 3(2):89–99.
11. Jaeger S, Karargyris A, Candemir S, Folio L, Sielgelman J, Callaghan F, Xue Z, Palaniappan K, Singh R, Antani S, Thoma G, Xiang Y-X, Lu P-X, McDonal C. Automatic tuberculosis screening using chest radiography. IEEE Transactions on Medical Imaging. 2013; 33(2):233–45.
12. Candemir S, Jaeger S, Palaniappan K, Musco JP. Lung segmentation in chest radiographs using anatomical atlases with nonrigid registration. IEEE Transactions on Medical Imaging. 2014; 33(2):577–90.
13. Agarwal R, Shankhadhar A, Sagar RK. Detection of lung cancer using content based medical image retrieval. 5th International Conference on Advanced Computing and Communication Technologies (ACCT). Haryana. 2015. p. 48–52.
14. Hadavi N, Nordin MJ, Shojaeipour A. Lung cancer diagnosis using CT-scan images based on cellular learning automata. International Conference on Computer and Information Sciences (ICCOINS). Malaysia. 2014. p. 1–5.
15. Armato SG, McLennan G, McNitt-Gray MF, Meyer CR, Yankelevitz D, Aberle DR, Henschke CI, Hoffman EA, Kazerooni EA, MacMahon H, Reeves A P, Croft BY, Clarke LP. Lung image database consortium: developing a resource for the medical imaging research community. Radiology. 2004; 232(3):739–48.
16. Messay T, Hardie RC, Rogers SK. A new computationally efficient CAD system for pulmonary nodule detection in CT imagery. Medical Image Analysis. 2010; 14 (3):390–406.